Immersed finite volume element methods for elliptic PDEs with interfaces and its application

Zhiyue Zhang

School of Mathematical Sciences, Nanjing Normal University
Email: zhangzhiyue@njnu.edu.cn

NNU · 南京师范大学
NANJING NORMAL UNIVERSITY

Modeling and simulation of interface dynamics in fluids/solids and their applications, May 14-18 2018, Singapore

Collaborators:

- Prof. Kazufumi ITO
- Prof. Zhilin LI
- Dr. Qian ZHANG
- Dr. Ling ZHU

We consider 2D elliptic interface problem on a rectangular domain Ω,

$$
\begin{align}
-\nabla \cdot \beta^{+}(x,y)\nabla u(x,y) = f(x,y) \quad (x,y) \in \Omega^{+}, \tag{1}\\
-\nabla \cdot \beta^{-}(x,y)\nabla u(x,y) = f(x,y) \quad (x,y) \in \Omega^{-}, \tag{2}
\end{align}
$$

where the interface $\Gamma \in C^2$ is a curve immersed in Ω, Ω^+ and Ω^- are sub-domains of Ω such that $\Omega^+ \cap \Omega^- = \emptyset$ and $\overline{\Omega^+} \cup \overline{\Omega^-} = \overline{\Omega}$. Along the interface, jump conditions for the solution and the flux are prescribed,

$$
[u]_\Gamma = w, \tag{3}
$$

$$
\left[\beta \frac{\partial u}{\partial \mathbf{n}}\right]_\Gamma = Q, \tag{4}
$$

The boundary condition is given as

$$
u(x,y) = g(x,y), \quad (x,y) \in \partial\Omega. \tag{5}
$$

Elliptic Interface problems

- J. Barrett, C. Elliott, **Fitted and unfitted FEM...**, IMA JNA, 1987.
- S. Chou, D. Kwak, K. Wee,**Optimal convergence analysis of IFEM...**, ACM., 2010
- T. Lin, Y. Lin, X. Zhang, **Partially penalized IFEM...**, SIAM JNA., 2015.
- R. Leveque, Z. Li, **The Immersed interface method...**, SIAM JNA. 1994.
- J. Bedrossian, J.H. Von Brecht, S. Zhu, E. Sifakis, J.M. Teran, **A second order virtual node method...**, JCP, 2010.
- R. Ewing, Z. Li, T. Lin, Y. Lin, **The Immersed FVEM...**, MCS.,1999.
- M. Oevermann, R. Klein, **A Cartesian grid FVM...**, JCP, 2006.
- Z. Li, K. Ito,**The immersed interface method: Numerical solutions...**, SIAM, Philadelphia, 2006

Our idea is using extension function to make interface problem with non-homogeneous jump conditions become one with homogeneous jump conditions. Those advantages are not only to use the usual finite element basis functions in trial space for different jump conditions, but also the scheme is simple and robust for the interface problem, and this method can be easily extended to solving other complex interface problems. we define

$$\hat{u}(x,y) = H(\varphi(x,y))u_\rho(x,y) = \begin{cases} 0 & \text{if } \varphi(x,y) < 0, \\ u_\rho(x,y) & \text{if } \varphi(x,y) \geq 0, \end{cases} \tag{6}$$

where $H(\cdot)$ is the Heaviside function. $\hat{u}(x,y)$ has the same non-homogeneous jumps conditions across the interface as $u(x,y)$

For an arbitrary interface Γ, there are three types of dual elements, as shown in Fig. 1.

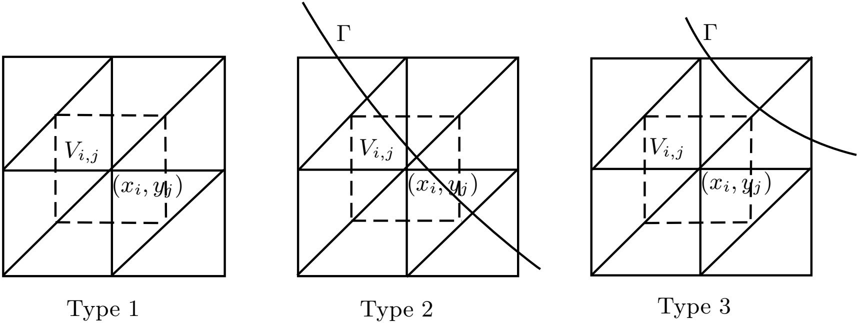

Figure: Three types of dual elements.

We integrate Equation of $q = u - \hat{u}$ on $V_{i,j}$ and have,

$$-\int_{V_{i,j}} \nabla \cdot \beta \nabla q dxdy = \int_{V_{i,j}} f dxdy + \int_{V_{i,j}} H(\varphi(x,y)) \nabla \cdot \beta \nabla u_\rho dxdy. \quad (7)$$

If $V_{i,j} \in \Omega^+$ or $\in \Omega^-$, then $V_{i,j}$ is Type 1 or Type 3, i.e. $V_{i,j} \cap \Gamma = \emptyset$. So we directly employ the Green's formula to obtain,

$$-\int_{\partial V_{i,j}} \beta \frac{\partial q}{\partial \mathbf{n}} ds = \int_{V_{i,j}} f dxdy + \int_{V_{i,j}} H(\varphi(x,y)) \nabla \cdot \beta \nabla u_\rho dxdy, \tag{8}$$

where $\mathbf{n}$ is the unit outward normal vector of $\partial V_{i,j}$.

If $V_{i,j}$ is Type 2, i.e. $V_{i,j} \cap \Gamma \neq \emptyset$, we need to apply the Green's formula piecewisely for the left hand side of (7),

$$
\begin{aligned}
-\int_{V_{i,j}} \nabla \cdot \beta \nabla q dxdy &= -\int_{V_{i,j}^{+}} \nabla \cdot \beta \nabla q dxdy - \int_{V_{i,j}^{-}} \nabla \cdot \beta \nabla q dxdy \qquad (9) \\
&= -\int_{\partial V_{i,j}} \beta \frac{\partial q}{\partial \mathbf{n}} ds - \int_{V_{i,j} \cap \Gamma} \left[\beta \frac{\partial q}{\partial \mathbf{n}} \right]_{\Gamma} ds.
\end{aligned}
$$

By the second jump condition $\left[\beta(x, y) \frac{\partial q}{\partial \mathbf{n}} \right]_{\Gamma} = 0$, we get the same scheme as (8).

We rewrite (7) in terms of $u = q + \hat{u}$ to obtain,

$$-\int_{\partial V_{i,j}} \beta \frac{\partial u}{\partial \mathbf{n}} ds = \int_{V_{i,j}} f(x,y)\, dxdy + \int_{V_{i,j}} H(\varphi(x,y)) \nabla \cdot \beta \nabla u_\rho \, dxdy - \int_{\partial V_{i,j}} \beta \frac{\partial \hat{u}}{\partial \mathbf{n}} ds. \quad (10)$$

If $V_{i,j} \in \Omega^-$, $H(\varphi(x,y)) = 0$, $\hat{u} = 0$.
If $V_{i,j} \in \Omega^+$, by applying Green's formula, we have

$$\int_{V_{i,j}} H(\varphi(x,y)) \nabla \cdot \beta \nabla u_\rho \, dxdy - \int_{\partial V_{i,j}} \beta \frac{\partial \hat{u}}{\partial \mathbf{n}} ds = 0. \quad (11)$$

Then, the numerical scheme is as follows:
If $V_{i,j}$ is Type 1 or Type 3, we have

$$-\int_{\partial V_{i,j}} \beta \left(\frac{\partial u_h}{\partial x} dy - \frac{\partial u_h}{\partial y} dx \right) = \int_{V_{i,j}} f(x, y) dxdy. \tag{12}$$

If $V_{i,j}$ is Type 2, we have

$$\begin{aligned} -\int_{\partial V_{i,j}} \beta \left(\frac{\partial u_h}{\partial x} dy - \frac{\partial u_h}{\partial y} dx \right) = \int_{V_{i,j}} f(x, y) dxdy \\ + \int_{V_{i,j}} H(\varphi(x, y)) \nabla \cdot \beta \nabla u_\rho dxdy - \int_{\partial V_{i,j}} \beta \left(\frac{\partial \hat{u}}{\partial x} dy - \frac{\partial \hat{u}}{\partial y} dx \right), \end{aligned} \tag{13}$$

However, if we treat Type 3 as above, the scheme is wrong. In the cell IV, $u_h \neq u_{i,j}\phi_{i,j} + u_{i+1,j}\phi_{i+1,j} + u_{i+1,j+1}\phi_{i+1,j+1}$, since these nodal basis functions only satisfy the homogeneous jump conditions as stated in the above definitions. We reconsider the schemes for the Type 3. If $V_{i,j} \in \Omega^-$, then $H(\varphi(x,y)) = 0$, thus from (8), we have

$$
\begin{aligned}
-\int_{\partial V_{i,j}} \beta \left(\frac{\partial u_h}{\partial x} dy - \frac{\partial u_h}{\partial y} dx \right) = \int_{V_{i,j}} f(x,y)\, dx dy \\
+ \sum_{(x_i,y_j) \in \mathcal{R}_{i,j}} H(\varphi(x_i,y_j)) A_{i,j} u_\rho(x_i,y_j),
\end{aligned}
\tag{14}
$$

where $A_{i,j} = -\int_{\partial V_{i,j}} \beta \left(\frac{\partial \phi_{i,j}}{\partial x} dy - \frac{\partial \phi_{i,j}}{\partial y} dx \right)$.

If $V_{i,j} \in \Omega^+$, then $H(\varphi(x,y)) = 1$. We get the scheme by using $u_h = q_h + \hat{u}$,

$$-\int_{\partial V_{i,j}} \beta \left(\frac{\partial u_h}{\partial x} dy - \frac{\partial u_h}{\partial y} dx \right) = \int_{V_{i,j}} f(x,y)\,dxdy \qquad (15)$$

$$+\int_{V_{i,j}} H(\varphi(x,y)) \nabla \cdot \beta \nabla u_\rho \,dxdy + \sum_{(x_i,y_j)\in\mathcal{R}_{i,j}} H(\varphi(x_i,y_j)) A_{i,j} u_\rho(x_i,y_j).$$

Theorem

Assume that T_h *is regular and* q *and* q_h *are the real solutions and numerical solution for the considered problem, respectively, and* $q \in \tilde{H}^2(\Omega)$, $\tilde{f} \in L^2(\Omega)$, *and* $\beta^s(x, y) \in W^{2,\infty}(\Omega^s)$ $(s = \pm)$, *then there exists* $C > 0$ *for* $h \in (0, h_0]$ *such that*

$$\|q - q_h\|_{1,h} \le Ch(\|q\|_2 + \|\tilde{f}\|). \tag{16}$$

Example

An example with an complicated interface and nonhomogeneous jump conditions.

The position of the interface is given in parametric form

$$X(\theta) = r(\theta)\cos(\theta) + x_0,$$

$$Y(\theta) = r(\theta)\sin(\theta) + y_0,$$

with $r(\theta) = r_0 + r_1\sin(\omega\theta),\ 0 \le \theta \le 2\pi$, where the parameters are set to $r_0 = 0.5,\ r_1 = 0.1,\ \omega = 5$, and $x_0 = y_0 = 0.2/\sqrt{20}$.
The coefficients $\beta^{\pm}$ and the solution $u^{\pm}$ are given as: (a) $\beta^{+} = 1000$, $\beta^{-} = 1$, (b) $\beta^{+} = 1$, $\beta^{-} = 1000$,

$$u^{+} = \frac{r^4 + C_0\log(2r)}{\beta^{+}},\ u^{-} = \frac{r^2}{\beta^{-}},$$

where $r = \sqrt{(x-x_0)^2 + (y-y_0)^2}$ and $C_0 = -0.1$.

Table: Convergence results for the solution u in the L^2, L^∞ and H^1 norm for Example 1.

Cases	Grids	e_∞	order1	e_0	order2	e_1	order
case(a)	64	3.88e-1		4.70e-2		1.28e+0	
$\beta^+ = 10^3$	128	1.15e-1	1.75	1.06e-2	2.14	4.69e-1	1.45
$\beta^- = 1$	256	2.42e-2	2.25	1.57e-3	2.76	1.62e-1	1.53
	512	8.09e-3	1.58	5.12e-4	1.61	8.22e-2	0.98
	1024	1.84e-3	2.14	8.99e-5	2.51	2.79e-2	1.56
case(b)	64	1.43e-2		1.18e-3		1.32e-1	
$\beta^+ = 1$	128	2.16e-3	2.72	1.02e-4	3.54	4.01e-2	1.72
$\beta^- = 10^3$	256	3.49e-4	2.63	1.90e-5	2.42	1.38e-2	1.54
	512	1.51e-4	1.21	5.46e-6	1.80	6.81e-3	1.02
	1024	2.13e-5	2.83	9.70e-7	2.49	2.29e-3	1.57

(a)

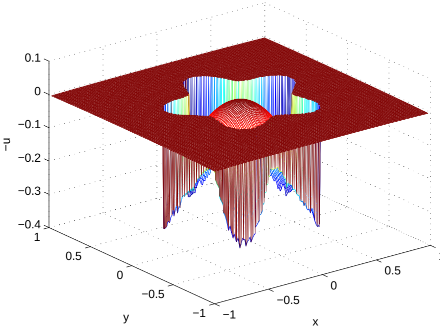

(b)

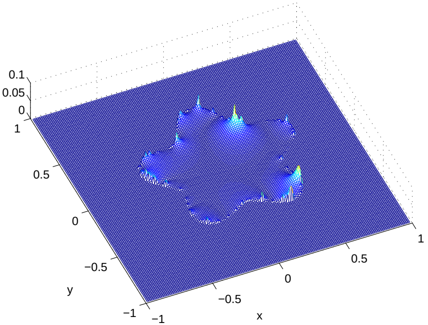

Figure: The figure of Example 1 with 160×160 grid-points: (a) is the numerical solution and (b) is the absolute error $|u - u_h|$ with $\beta^+/\beta^- = 1000$, respectively.

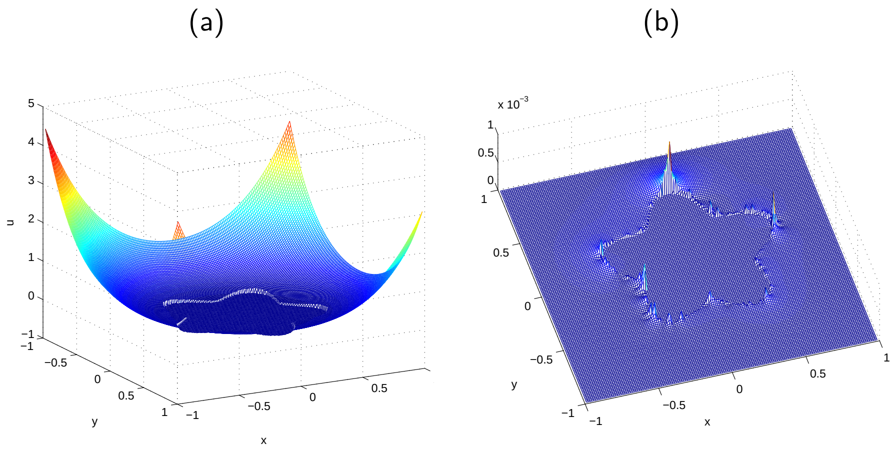

Figure: The figure of Example 1 with 160×160 grid-points: (a) is the numerical solution and (b) is the absolute error $|u - u_h|$ with $\beta^+/\beta^- = 1/1000$, respectively.

Example

An interface problem with homogeneous jump conditions.

The level-set function φ, the coefficients $\beta^{\pm}$, and the solution $u^{\pm}$ are given as follows: $\varphi = x^2 + y^2 - 0.25$, (a) $\beta^+ = 1000$, $\beta^- = 1$, (b) $\beta^+ = 1$, $\beta^- = 1000$,

$$u(x, y) = \begin{cases} u^+ = \dfrac{r^\alpha}{\beta^+} + \left(\dfrac{1}{\beta^-} - \dfrac{1}{\beta^+}\right) r_0^\alpha, & \text{if } r \geq r_0, \\ u^- = \dfrac{r^\alpha}{\beta^-}, & \text{otherwise}, \end{cases}$$

with $\alpha = 5$, $r = \sqrt{x^2 + y^2}$, $r_0 = 0.5$.

Table: Convergence results for the solution u in the L^2, L^∞ and H^1 norm for Example 2.

Cases	Grids	e_∞	order1	e_0	order2	e_1	order3
case(a)	64	2.97e-4		6.84e-5		6.79e-3	
$\beta^+ = 10^3$	128	6.73e-5	2.14	1.52e-5	2.17	3.46e-3	0.97
$\beta^-=1$	256	2.70e-5	1.32	4.21e-6	1.86	1.75e-3	0.98
	512	7.27e-6	1.89	1.34e-6	1.66	8.79e-4	0.99
	1024	2.34e-6	1.63	3.36e-7	1.99	4.40e-4	1.00
case(b)	64	9.40e-4		9.56e-4		1.99e-1	
$\beta^+ = 1$	128	2.13e-4	2.15	2.34e-4	2.03	1.06e-1	0.91
$\beta^- = 10^3$	256	5.98e-5	1.83	5.95e-5	1.98	5.48e-2	0.95
	512	1.40e-5	2.10	1.42e-5	2.06	2.78e-2	0.98
	1024	3.59e-6	1.96	3.61e-6	1.98	1.40e-2	0.99

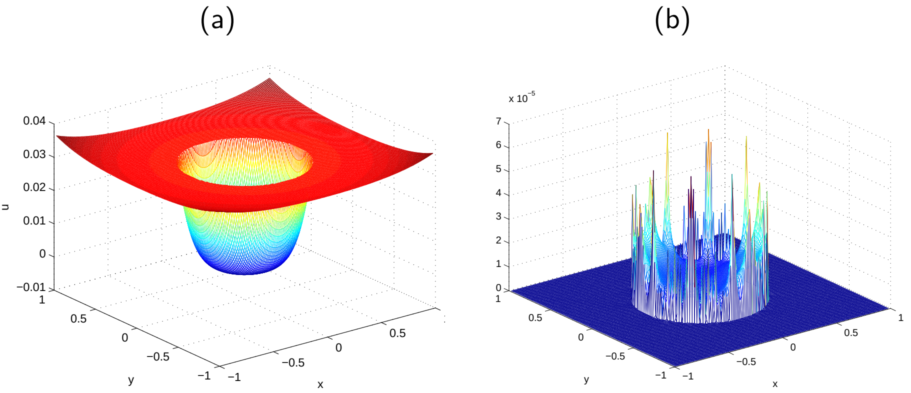

Figure: The figure of Example 2 with 160×160 grid-points: (a) is the numerical solution and (b) is the absolute error $|u - u_h|$ with $\beta^+/\beta^- = 1000$, respectively.

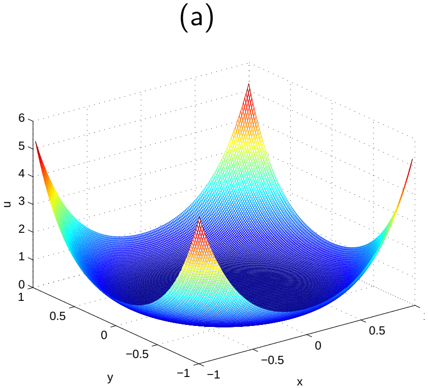

Figure: The figure of Example 2 with 160×160 grid-points: (a) is the numerical solution and (b) is the absolute error $|u - u_h|$ with $\beta^+/\beta^- = 1/1000$, respectively.

A stabilized immersed finite volume element (SIFVE) schemes for interface problem: Find $u_h \in \widehat{S}_h(\Omega)$ such that

$$\tilde{a}_h(u_h, I_h^* v_h) = (f, I_h^* v_h), \quad \forall v_h \in \widehat{S}_h(\Omega), \tag{17}$$

where

$$\tilde{a}_h(u_h, I_h^* v_h) = -\sum_{V_i} I_h^* v_h \int_{\partial V_i} \beta \nabla u_h \cdot \mathrm{n}\, ds + \sum_{e \in \mathcal{E}_h^i} \int_e \frac{\sigma}{h} [u_h][v_h]\, ds.$$

Table: Errors of classic IFVE when $\beta^- = 1$ and $\beta^+ = 1000$.

h	L^∞ error	r	L^2 error	r	H^1 error	r
$1/32$	2.9948E-04	-	7.2651E-05	-	9.2961E-03	-
$1/64$	6.8083E-05	2.14	1.6338E-05	2.15	5.0791E-03	0.87
$1/128$	2.6917E-05	1.34	4.5134E-06	1.86	2.6386E-03	0.94
$1/256$	7.2802E-06	1.89	1.4366E-06	1.65	1.3448E-03	0.97
$1/512$	2.3432E-06	1.64	3.6131E-07	1.99	6.7922E-04	0.99

Table: Errors of SIFVE when $\beta^- = 1$ and $\beta^+ = 1000$.

h	L^∞ error	r	L^2 error	r	H^1 error	r
$1/32$	2.3694E-04	-	8.8773E-05	-	9.4078E-03	-
$1/64$	6.9202E-05	1.78	1.8250E-05	2.28	5.0933E-03	0.89
$1/128$	2.1526E-05	1.68	5.1709E-06	1.82	2.6449E-03	0.95
$1/256$	5.7431E-06	1.91	1.5637E-06	1.73	1.3462E-03	0.97
$1/512$	1.7438E-06	1.72	3.9675E-07	1.98	6.7960E-04	0.99

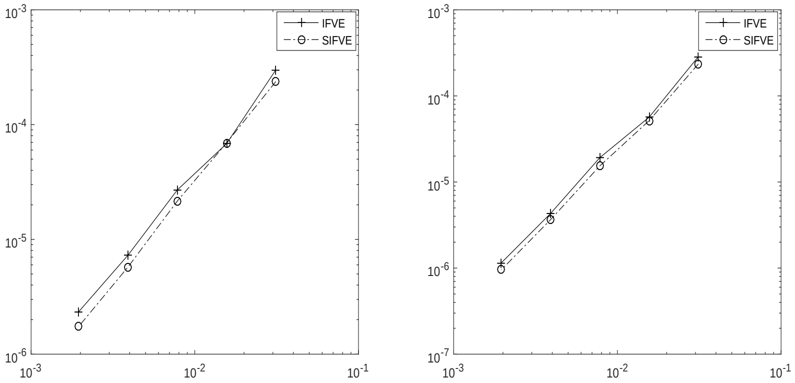

Figure: The L^∞ error under uniform refinement of the mesh for $\beta^-/\beta^+ = 1/1000$ (left) and $\beta^-/\beta^+ = 1/10$ (right).

Consider the stochastic elliptic interface problem: Find a random function, $u : \Omega \times D \to \mathbb{R}$, such that P-almost everywhere in probability Ω, or in other words, almost surely, the following equation holds:

$$
\begin{aligned}
&-\nabla \cdot (\beta(\omega,\cdot)\nabla u(\omega,\cdot)) = f(\omega,\cdot) && \text{in } D^+ \cup D^-, && (18)\\
&[u(\omega,\cdot)]_\Gamma = 0 \quad \left[\beta(\omega,\cdot)\frac{\partial u(\omega,\cdot)}{\partial \mathbf{n}}\right]_\Gamma = 0 && \text{on } \Gamma, && (19)\\
&u = 0 && \text{on } \partial D. && (20)
\end{aligned}
$$

The coefficient $\beta(\omega, \mathbf{x}) : \Omega \times D \to \mathbb{R}$ is a piecewise random function, that is,

$$
\beta(\omega,\mathbf{x}) = \begin{cases} \beta^-(\omega,\mathbf{x}) & \mathbf{x} \in D^-, \\ \beta^+(\omega,\mathbf{x}) & \mathbf{x} \in D^+. \end{cases} \tag{21}
$$

In addition, we shall make the following assumptions of the data:

1. The coefficient $\beta(\omega, \cdot)$ is uniformly bounded and coercive, i.e., there exist $\beta_{min},\ \beta_{max} \in (0,\ \infty)$ such that $P\left\{\omega \in \Omega :\ \beta(\omega, \mathbf{x}) \in [\beta_{min},\ \beta_{max}],\ \forall \mathbf{x} \in D\right\} = 1$;
2. For any $\omega \in \Omega$, the function $f(\omega,\ \cdot)$ belongs to the space $L^2(D)$ and is square integrable with respect to P in the sense of

$$\int_\Omega \|f(\omega, \cdot)\|^2_{L^2(D)} dP(\omega) < \infty.$$

The weak form of the problem (18)-(20): Find $u \in L^2_P(\Omega) \otimes H^1_0(D)$ such that

$$\int_D \mathbb{E}[\beta \nabla u \cdot \nabla v] d\mathbf{x} = \int_D \mathbb{E}[fv] d\mathbf{x} \quad \text{for all } v \in L^2_P(\Omega) \otimes H^1_0(D). \tag{22}$$

where $\mathbb{E}[\cdot]$ stands for the expectation. Moreover, we have the following regularity result for the problem with respect to $\mathbf{x}$ [J. H. Bramble and J. T. King, 1996]. The solution to (22) has realizations in the space $\widetilde{H}^2(D)$, i.e., for any $\omega \in \Omega$, $u(\omega, \cdot) \in \widetilde{H}^2(D)$ and

$$\|u(\omega, \cdot)\|_{\widetilde{H}^2(D)} \leq C \|f(\omega, \cdot)\|_{L^2(D)}$$

.

Let the mean and the covariance of $\beta^{\pm}(\omega, \mathbf{x})$ be defined as

$$\beta_0^{\pm}(\mathbf{x}) = \int_{\Omega} \beta^{\pm}(\omega, \mathbf{x}) dP, \qquad \forall \mathbf{x} \in D^{\pm} \tag{23}$$

and

$$Cov_{\beta^{\pm}}(\mathbf{x}, \mathbf{x}_1) = \int_{\Omega} \left(\beta^{\pm}(\omega, \mathbf{x}) - \beta_0^{\pm}(\mathbf{x})\right) \left(\beta^{\pm}(\omega, \mathbf{x}_1) - \beta_0^{\pm}(\mathbf{x}_1)\right) dP, \tag{24}$$

respectively. Then the Karhunen-Loève (KL) expansion of $\beta^{\pm}(\omega, \mathbf{x})$ is

$$\beta^{\pm}(\omega, \mathbf{x}) = \beta_0^{\pm}(\mathbf{x}) + \sum_{n=1}^{\infty} \sqrt{\lambda_n^{\pm}} \beta_n^{\pm}(\mathbf{x}) y_n^{\pm}(\omega), \tag{25}$$

where $\beta_n^{\pm}$ are the orthogonal and normalized eigenfunctions and $\lambda_n^{\pm}$ are the corresponding eigenvalues of the following eigenvalue problem

$$\int_{D^{\pm}} Cov_{\beta^{\pm}}(\mathbf{x}, \mathbf{x}_1) \beta_n^{\pm}(\mathbf{x}_1) d\mathbf{x}_1 = \lambda_n^{\pm} \beta_n^{\pm}(\mathbf{x}). \tag{26}$$

It is shown in [R. G. Ghanem and P. D. Spanos, 1991] that the Karhunen-Loève expansion is optimal among all possible representations of random processes in the sense of the mean-square error. The truncated Karhunen-Loève expansion reads

$$\beta^{\pm}_{N^{\pm}}(\omega, \mathbf{x}) = \beta^{\pm}_0(\mathbf{x}) + \sum_{n=1}^{N^{\pm}} \sqrt{\lambda^{\pm}_n}\beta^{\pm}_n(\mathbf{x}) y^{\pm}_n(\omega). \tag{27}$$

Theorem

(Finite-dimensional noise) The coefficients in the original equation have the form

$$\beta^{\pm}(\omega,\mathbf{x}) = \beta^{\pm}\left(y_1^{\pm}(\omega), y_2^{\pm}(\omega), \cdots, y_{N^{\pm}}^{\pm}(\omega), \mathbf{x}\right) = \beta_0^{\pm}(\mathbf{x}) + \sum_{n=1}^{N^{\pm}} \sqrt{\lambda_n^{\pm}}\beta_n^{\pm}(\mathbf{x}) y_n^{\pm}$$

where $N^{\pm}$ are positive integers, $\{y_n^{\pm}\}_{n=1}^{N^{\pm}}$ are real-valued and independent random variables with mean value zero and unit variance. The function f has a similar form $f(\omega,\mathbf{x}) = f(y_1^f(\omega), \cdots, y_{N^f}^f(\omega), \mathbf{x})$. Define $\mathbf{y} = (y_1, \cdots, y_N) = (y_1^+, \cdots, y_{N^+}^+, y_1^-, \cdots, y_{N^-}^-, y_1^f, \cdots, y_{N^f}^f)$ with $N = N^+ + N^- + N^f$, we can rewrite $\beta^{\pm}(\omega,\mathbf{x}) = \beta^{\pm}(\mathbf{y},\mathbf{x})$ and $f(\omega,\mathbf{x}) = f(\mathbf{y},\mathbf{x})$.

Under the finite-dimensional assumption, the stochastic problem (18)-(20) now becomes a deterministic elliptic interface problem with N-dimensional parameter, i.e., find $u(\mathbf{y},\mathbf{x}) : \Theta \times D \to \mathbb{R}$, for all $\mathbf{y} \in \Theta$, the following holds

$$\begin{cases} -\nabla \cdot (\beta(\mathbf{y},\mathbf{x})\nabla u(\mathbf{y},\mathbf{x})) = f(\mathbf{y},\mathbf{x}) & \mathbf{x} \in D^+ \cup D^-, \\ [u(\mathbf{y},\mathbf{x})]_\Gamma = 0 \quad \left[\beta \dfrac{\partial u(\mathbf{y},\mathbf{x})}{\partial \mathbf{n}}\right]_\Gamma = 0 & \mathbf{x} \in \Gamma, \\ u(\mathbf{y},\mathbf{x}) = 0 & \mathbf{x} \in \partial D. \end{cases} \tag{28}$$

The stochastic variational formulation (22) has a deterministic equivalent: Find $u(\mathbf{y},\mathbf{x}) \in L^2_\rho(\Theta) \otimes H^1_0(D)$ such that

$$\int_{\Theta\times D} \rho(\mathbf{y})\beta(\mathbf{y},\mathbf{x})\nabla u(\mathbf{y},\mathbf{x})\cdot\nabla v(\mathbf{y},\mathbf{x})\,d\mathbf{y}\,d\mathbf{x} = \int_{\Theta\times D} \rho(\mathbf{y})f(\mathbf{y},\mathbf{x})v(\mathbf{y},\mathbf{x})\,d\mathbf{y}\,d\mathbf{x}, \tag{29}$$

In the stochastic collocation method, we first evaluate approximation functions $u_h(\mathbf{y}_k, \cdot) \in S_h(D)$ to the solution of (28) on a suitable set of points $\mathbf{y}_k \in \Theta$ using the immersed finite element method. Then the fully discrete solution $u_{h,\mathbf{p}} \in C^0(\Theta; S_h(D))$ is a polynomial interpolation in the random space, i.e.,

$$u_{h,\mathbf{p}}(\mathbf{y}, \mathbf{x}) = \sum_k u_h(\mathbf{y}_k, \mathbf{x}) l_k^{\mathbf{p}}(\mathbf{y}), \tag{30}$$

where, for instance, the functions $l_k^{\mathbf{p}}$ can be taken as the Lagrange polynomials. Then the approximation of the expected value of u to the stochastic equation (18)-(20) can be evaluated as

$$\mathbf{E}[u] \approx \mathbf{E}[u_{h,\mathbf{p}}] = \sum_k u_h(\mathbf{y}_k, \mathbf{x}) \int_\Theta \rho(\mathbf{y}) l_k^{\mathbf{p}}(\mathbf{y}) d\mathbf{y}. \tag{31}$$

First we assume $N = 1$, and let $\{y_1^i, \cdots, y_{m_i}^i\} \subset \Theta$ be a sequence of abscissas for Lagrange interpolation. Here the integer i means the level of approximation and m_i is the number of interpolation points used at level i. Then, the one-dimensional Lagrange interpolation is

$$\mathcal{U}^i(u) = \sum_{k=1}^{m_i} u(y_k^i) l_k^i, \tag{32}$$

where $l_k^i \in \mathcal{P}_{m_i-1}(\Theta)$ are the Lagrange polynomials of degree $m_i - 1$, i.e., $l_k^i(y) = \prod_{k=1,k\neq j}^{m_i} \frac{(y-y_k^i)}{(y_j^i - y_k^i)}$. In the multi-dimensional case, i.e., $N > 1$, the Lagrange interpolation based on the full tensor product is defined by

$$\mathcal{I}_{\mathbf{i}}^N(u)(\mathbf{y}) = (\mathcal{U}^{i_1} \otimes \cdots \otimes \mathcal{U}^{i_N})(u)(\mathbf{y}) = \sum_{j_1=1}^{m_{i_1}} \cdots \sum_{j_N=1}^{m_{i_N}} u(y_{j_1}^{i_1}, \cdots, y_{j_N}^{i_N})(l_{j_1}^{i_1} \otimes \cdots \otimes l_{j_N}^{i_N} \tag{33}$$

Now we briefly describe the isotropic Smolyak formulation which is a linear combination of low order tensor product formula (33). The Smolyak formula is then given by

$$\mathcal{A}(w,N)=\sum_{w+1\le|\mathbf{i}|\le w+N}(-1)^{w+N-|\mathbf{i}|}\left(\begin{array}{c}N-1\\ w+N-|\mathbf{i}|\end{array}\right)(\mathcal{U}^{i_1}\otimes\cdots\otimes\mathcal{U}^{i_N}), \tag{34}$$

where $\mathbf{i}\in\mathbb{N}_+^N$ and $|\mathbf{i}|=i_1+\cdots+i_N$. The set of the sparse grids needed to compute $\mathcal{A}(w,N)(u)$ is

$$\mathcal{H}(w,N)=\sum_{w+1\le|\mathbf{i}|\le w+N}(\vartheta^{i_1}\times\cdots\times\vartheta^{i_N}), \tag{35}$$

where $\vartheta^i=\{y_1^i,\cdots,y_{m_i}^i\}$ is the set of abscissas used by $\mathcal{U}^i$.
We choose to use Clenshaw-Curtis abscissas which are the extreme of Chebyshev polynomials, that is, for any choice of $m_i>1$,

$$y_j^i=-\cos\frac{\pi(j-1)}{m_i-1},\ j=1,\cdots,m_i. \tag{36}$$

In addition, we define $y_1^i=0$ if $m_i=1$, and choose $m_1=1$ and $m_i=2^{i-1}+1$ for $i>1$.

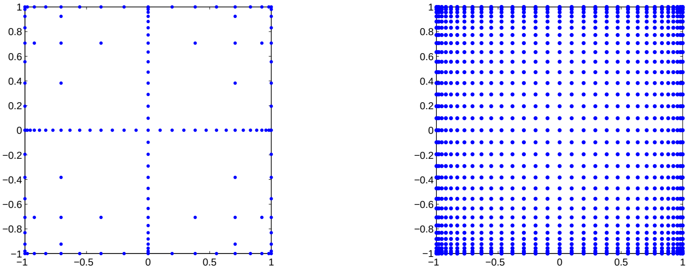

Fig.1: Two-dimensional (N=2) interpolation nodes based on the extreme of Chebyshev polynomials (36). Left: sparse grids $\mathcal{H}(w, N)$ with $w = 5$. Total number of points is 145. Right: the tensor product grids based on the same one-dimensional nodes. Total number of nodes is 1089.

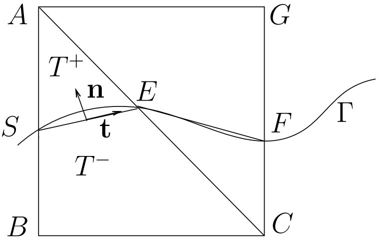

Fig.2: A typical interface element and a neighboring element.

We take a typical interface element $\triangle ABC$ whose geometric configuration is given in Figure 8 as a demonstration. The line segment $\overline{SE}$ divides T into two parts T^+ and T^-. Let **n** and **t** be the unit normal and tangential directions of the line segment $\overline{SE}$, respectively. We construct the following piecewise linear function on this element,

$$\phi(\mathbf{x}) = \begin{cases} \phi^+ = a^+ + b^+ x_1 + c^+ x_2, & \mathbf{x} = (x_1, x_2) \in T^+, \\ \phi^- = a^- + b^- x_1 + c^- x_2, & \mathbf{x} = (x_1, x_2) \in T^-. \end{cases} \tag{37}$$

The coefficients are chosen such that

$$\phi(A) = V_1,\ \phi(B) = V_2,\ \phi(C) = V_3, \tag{38}$$

$$\phi^+(S) = \phi^-(S),\ \phi^+(E) = \phi^-(E),\ \beta^+\frac{\partial\phi^+}{\partial \mathbf{n}} = \beta^-\frac{\partial\phi^-}{\partial \mathbf{n}}, \tag{39}$$

where $V_i,\ i = 1, 2, 3$ are the nodal variables. Intuitively, there are six unknowns in (70) and six restrictions in (71)-(72). The piecewise linear function is uniquely determined by $V_i,\ i = 1, 2, 3.$

Definition

(IFE space) The IFE space $V_h^J(\Omega)$ is defined as the set of all piecewise linear functions that satisfy

- $\phi|_T$ is the linear function if T is the non-interface element
- $\phi|_T$ is the piecewise linear function defined in (70)-(72) if T is the interface element
- ϕ is continuous at all nodal points,
- $\phi(\mathbf{x}_b) = 0$ if $\mathbf{x}_b$ is a nodal point on $\partial\Omega$.

For any $\mathbf{y} \in \Theta$, the immersed finite element approximation of (28) reads: Find $u_h(\mathbf{y}, \cdot) \in S_h(D)$ such that

$$a_h(u_h(\mathbf{y}, \mathbf{x}), v(\mathbf{x})) = \int_D f(\mathbf{y}, \mathbf{x}) v(\mathbf{x}) d\mathbf{x}, \qquad \forall v(\mathbf{x}) \in S_h(D), \tag{40}$$

where the bilinear form $a_h(\cdot, \cdot)$ is defined by

$$a_h(w, v) = \sum_{T \in \mathcal{T}_h} \int_T \beta \nabla w \cdot \nabla v d\mathbf{x}, \qquad \forall w, v \in S_h(D). \tag{41}$$

It has been proven that the immersed finite element method has the optimal convergence order in L^2-norm, that is,

$$\|u(\mathbf{y}, \cdot) - u_h(\mathbf{y}, \cdot)\|_{L^2(D)} \leq Ch^2 \|u(\mathbf{y}, \cdot)\|_{\widetilde{H}^2(D)}, \qquad \forall \mathbf{y} \in \Theta. \tag{42}$$

We recall that u is the solution of the original stochastic problem (18)-(20), u_h is the semidiscrete approximation obtained by the IFEM and $\mathcal{A}(w,N)u_h$ is the fully discrete numerical solution. The error to be considered can be split as

$$\|u-\mathcal{A}(w,N)u_h\|_{L^2_\rho(\Theta)\otimes L^2(D)} \leq \|u-u_h\|_{L^2_\rho(\Theta)\otimes L^2(D)}+\|u_h-\mathcal{A}(w,N)u_h\|_{L^2_\rho(\Theta)\otimes} \tag{43}$$

The first term is nothing but the approximation error in physical spaces, i.e., the error of the IFEM. By [S. Chou, D. Y. Kwak, and K. T. Wee, 2010], we have

$$\begin{aligned}\|u-u_h\|_{L^2_\rho(\Theta)\otimes L^2(D)} &= \left(\int_\Theta \int_D \rho|u(\mathbf{y},\mathbf{x})-u_h(\mathbf{y},\mathbf{x})|^2 d\mathbf{x}d\mathbf{y}\right)^{1/2} \\ &\leq Ch^2\|u\|_{L^2_\rho(\Theta)\otimes\widetilde{H}^2(D)}.\end{aligned} \tag{44}$$

The second term is the Smolyak approximation error. To estimate the approximation error, we first give the following lemma [F. Nobile, A. Clement, F. Moës, 2008. Theorem 3.10].

Lemma

Let $\Theta^* = \prod_{j=1, j\neq n}^{N} \Theta_j$ *and* y_n^* *be an arbitrary element of* Θ^**. For each* $y_n \in \Theta_n$*, assume that there exists* τ_n *such that* $u(y_n, y_n^*, \mathbf{x})$ *as a function of* y_n *admits an analytic extension* $u(z, y_n^*, \mathbf{x})$*,* $z \in \mathbb{C}$*, in the region of the complex plane*

$$\sigma(\Theta_n; \tau_n) = \{z \in \mathbb{C}, dist(z, \Theta_n) \leq \tau_n\}. \tag{45}$$

Also define the parameter

$$\sigma = \frac{1}{2} \min_{n=1,\cdots,N} \log\left(\frac{2\tau_n}{|\Theta_n|} + \sqrt{1 + \frac{4\tau_n^2}{|\Theta_n|^2}}\right). \tag{46}$$

Then the isotropic Smolyak formula (34) based on Clenshaw-Curtis abscissas satisfies

$$\|u - \mathcal{A}(w, N)(u)\|_{L^\infty(\Theta^N; W_h(D))} \leq C(\sigma, N)\eta^{-\mu_1} \text{ with } \mu_1 = \frac{\sigma}{1 + \log(2N)}, \tag{47}$$

where $\eta = |\mathcal{H}(w, N)|$ *is the number of collocation points*

However u_h is required to satisfy the regularity assumption made in the above lemma. It has been proved in [I. Babuška, F. Nobile and R. Tempone, 2010. Lemma 3.2] that the problem satisfies the regularity assumption with $0 < \tau_n < 1/(2/\gamma_n)$ if the following holds:

$$\left\| \frac{\partial_{y_n}^k \beta(\mathbf{y}, \cdot)}{\beta(\mathbf{y}, \cdot)} \right\|_{L^\infty(D)} \leq \gamma_n^k k! \quad \frac{\|\partial_{y_n}^k f(\mathbf{y}, \cdot)\|_{L^2(D)}}{1 + \|f(\mathbf{y}, \cdot)\|_{L^2(D)}} \leq \gamma_n^k k!. \tag{48}$$

Under the assumption 4, we have

$$\frac{\partial_{y_n}^k \beta^+(\mathbf{y}, \mathbf{x})}{\beta(\mathbf{y}, \mathbf{x})} \leq \begin{cases} \sqrt{\lambda_n} \beta_n^+(\mathbf{x})/\beta_{min} & \text{if } k = 1 \\ 0 & \text{if } k > 1 \text{ or } n > N^+ \end{cases} \tag{49}$$

and similar results for β^- and f. Thus (48) is satisfied if we take $\gamma_n = \sqrt{\lambda_n} \|\beta_n^+\|_{L^\infty(D^+)}/\beta_{min}$ for $n = 1, \cdots, N^+$. For the case of $n > N^+$, the constant γ_n can be chosen similarly. Note that the regularity results are valid also for the semidiscrete solution u_h.

Using Lemma 6, the second term now can be estimated, we have

Theorem

Under the assumption 4, it holds that

$$\|u-\mathcal{A}(w,N)u_h\|_{L^2_\rho(\Theta)\otimes L^2(D)} \le Ch^2\|u\|_{L^2_\rho(\Theta)\otimes \widetilde{H}^2(D)}+C(\sigma,N)\eta^{-\sigma/(1+\log(N))}, \tag{50}$$

where σ is defined in (46) and the constants C and $C(\sigma,N)$ are independent of h and η.

Using the theorem, the error in the expected value of u is easily estimated, i.e.,

$$\begin{aligned}\|\mathbb{E}[u]-\mathbb{E}[\mathcal{A}(w,N)u_h]\|_{L^2(D)} &\le \|u-\mathcal{A}(w,N)u_h\|_{L^2_\rho(\Theta)\otimes L^2(D)}\\ &\le Ch^2\|u\|_{L^2_\rho(\Theta)\otimes \widetilde{H}^2(D)}+C(\sigma,N)\eta^{-\sigma/(1+\log(N))}\end{aligned} \tag{51}$$

For simplicity, the problems are defined in the rectangular domain $D = [-1,1] \times [-1,1]$ which is partitioned into $2N_h^2$ right triangles with mesh size h. We consider a deterministic right-hand function f and construct the random coefficient as

$$\beta(\mathbf{y},\mathbf{x}) = \begin{cases} \beta^-(\mathbf{y},\mathbf{x}) = \beta_0^-(\mathbf{x})(1 + 0.5 * \sum_{n=1}^{M} \frac{1}{n^2} y_n), & \mathbf{x} \in D^-, \\ \beta^+(\mathbf{y},\mathbf{x}) = \beta_0^+(\mathbf{x})(1 + 0.5 * \sum_{n=M+1}^{2M} \frac{1}{n^2} y_n), & \mathbf{x} \in D^+, \end{cases} \tag{52}$$

with $N = 2M$ the dimension of random space, and $y_n \in [-1,1]$, $n = 1, \cdots, N$, are independent uniformly distributed random variables. In all examples, we compute the $L^2(D)$ error to the expected value, i.e.,

$$\text{Error} = \|\mathbb{E}[u] - \mathbb{E}[\mathcal{A}(w,N)u_h]\|_{L^2(D)}, \tag{53}$$

where the expected value of exact solution is approximated as $\mathbb{E}[u] \approx \mathbb{E}[\mathcal{A}(\widetilde{w},N)u_h]$ with a larger $\widetilde{w}$.

The interface Γ is a circle centered at the origin with radius $r_0 = 0.5$, as shown in Figure 9. The true solution is

$$u = \begin{cases} \dfrac{r^3}{\beta^-} & \text{in } D^-, \\ \dfrac{r^3}{\beta^+} + (\dfrac{1}{\beta^-} - \dfrac{1}{\beta^+})r_0^3 & \text{in } D^+. \end{cases} \tag{54}$$

where $r = \sqrt{x_1^2 + x_2^2}$. In this example, we choose $\beta_0^+ = 100$ and $\beta_0^- = 1$ in (52).

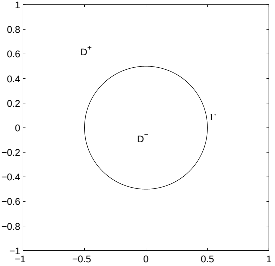

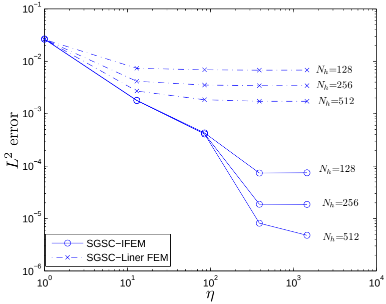

(a) L^2 error versus the number of collocation points η

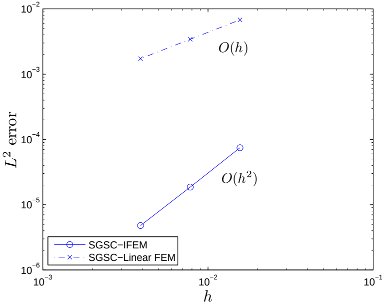

(b) L^2 error versus the mesh-spacing parameter h with $w = 4$

Fig.4: A comparison between the sparse grid stochastic collocation (SGSC) method based on the IFEM and the standard linear FEM for solving Example 1 with N=6.

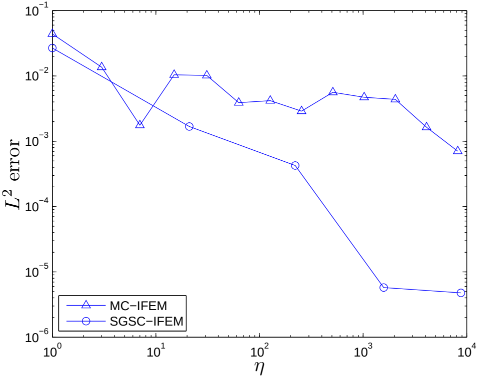

Fig.5: A comparison between the sparse grid stochastic collocation method and the Monte Carlo approach for solving Example 1 with N=10 and $N_h = 512$.

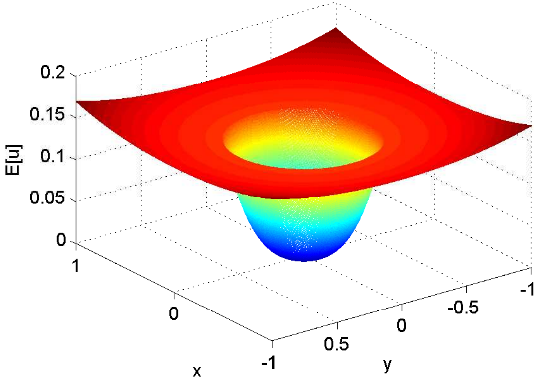

Fig.6: The exact expectation of Example 1 with N=10.

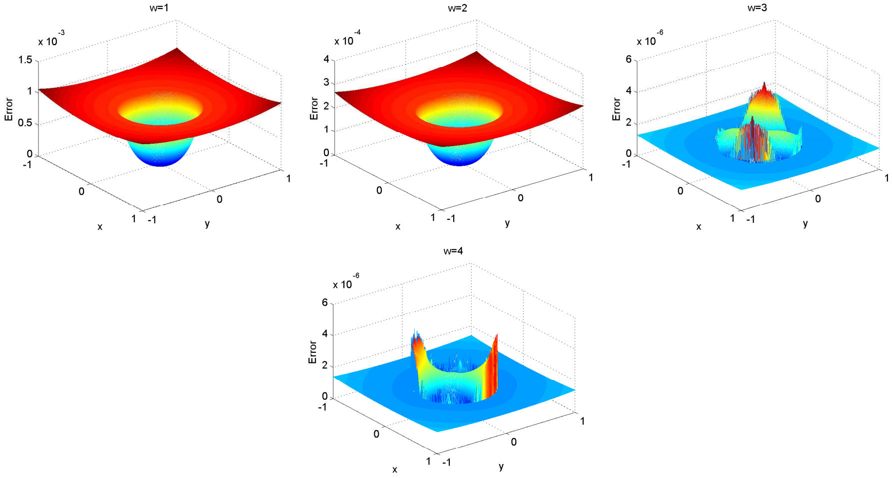

Fig.7: The error distribution of the expected value of Example 1 with N=10 and w=1, 2, 3, 4.

The interface is the zero level set of the function is $\varphi(x_1, x_2) = -x_2^2 + ((x_1 - 1)\tan\theta)^2 x_1$, where θ is a parameter. The interface has a corner of angle 2θ at (1, 0) as shown in Figure 14. The exact solution is chosen as $u = \varphi(x_1, x_2)/\beta$. It is easy to verify that the solution indeed satisfies the PDE and the jump conditions using the fact of $\mathbf{n} = \nabla\varphi/|\nabla\varphi|$. In this case, we choose $\beta_0^- = 1$ and $\beta_0^+ = 10$ in (52). The dimension of random space is set to be $N = 10$.

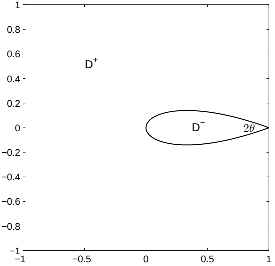

Fig.8: The domain and the interface of Example 2. The interface has a corner of angle 2θ at (1, 0).

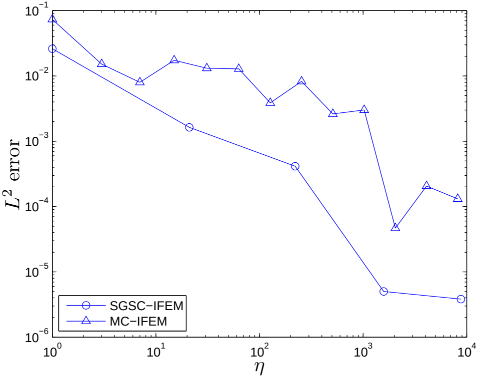

Fig.9: A comparison between the SGSC-IFEM and the MC-IFEM for solving Example 2 with N=10.

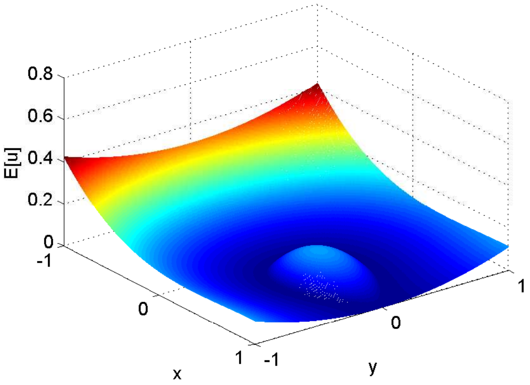

Fig.10: The expected value of Example 2 with N=10.

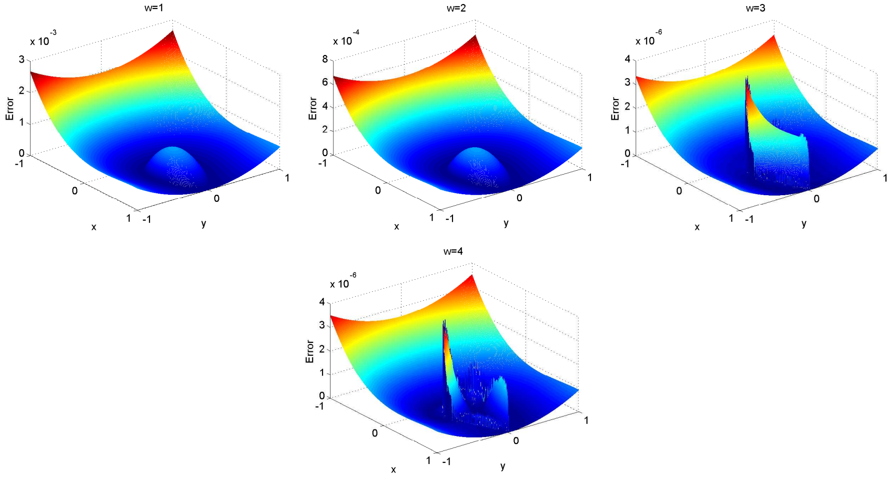

Fig.11: The error distribution of the expected value of Example 2 with N=10 and w=1, 2, 3, 4.

We consider the case where β_0^+ and β_0^- in (52) is not a piecewise constant,

$$\begin{cases} \beta_0^+ = 1 & \text{in } D^+, \\ \beta_0^- = 10 + 5(x_1^2 - x_1x_2 + x_2^2) & \text{in } D^-. \end{cases} \tag{55}$$

The interface is the zero level set of $\varphi(x_1, x_2) = x_1^2/(0.5^2) + x_2^2/(0.25)^2 - 1$. The exact solution is chosen as $u = \varphi(x_1, x_2)/\beta$. And we set $N = 8$.

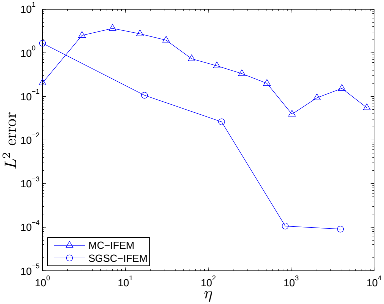

Fig.12: A comparison between the SGSC-IFEM and the MC-IFEM for solving Example 3 with N=8.

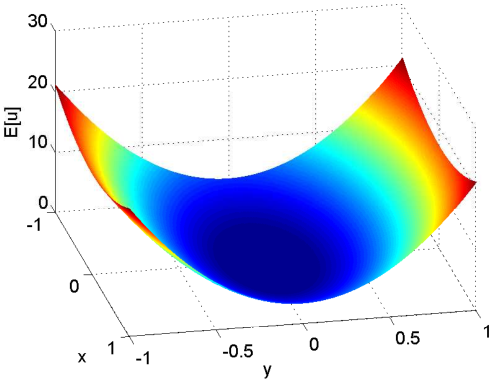

Fig.13: The expected value of Example 3 with N=8.

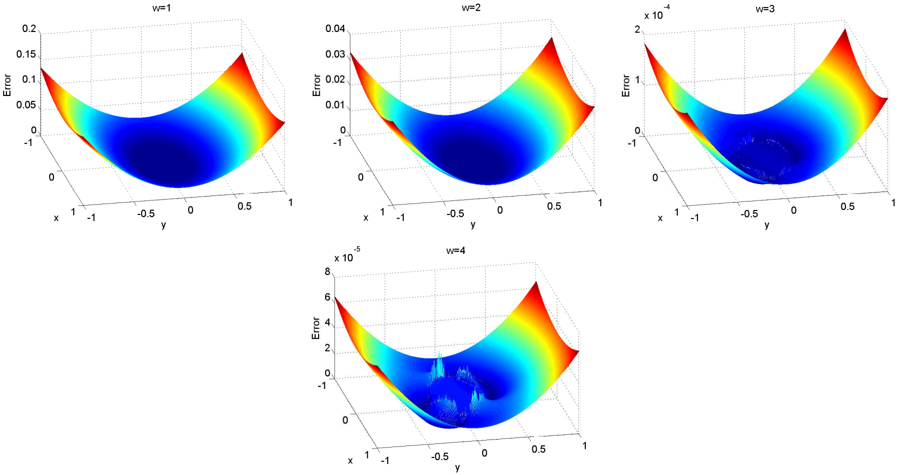

Fig.14: The error distribution of the expected value of Example 3 with N=8 and w=1, 2, 3, 4.

We have presented a stochastic collocation method for the numerical solution of elliptic partial differential equations with both random inputs and interfaces.

To relieve the *curse of dimensionality*, we use the sparse grid collocation method based on the isotropic Smolyak construction instead of using the full tensor product construction.

In the error analysis, we divide the error into two parts and provide the error estimates respectively. Numerical examples have shown that the sparse grid collocation method preserves a high level of accuracy and it is a valid alternative to the more traditional Monte Carlo method.

Consider the elliptic interface equation

$$-\nabla \cdot (\beta(\mathbf{x})\nabla y(\mathbf{x})) = u(\mathbf{x}) \quad \text{in } \Omega\backslash\Gamma, \tag{56}$$

$$[y]_\Gamma = 0, \ \ [\beta \partial_{\mathbf{n}} y]_\Gamma = 0, \tag{57}$$

$$y = 0 \quad \text{on } \partial\Omega, \tag{58}$$

$[y]_\Gamma$: the jump of the function $y(\mathbf{x})$ across the interface Γ;
Γ: the interface which separates the domain Ω into two sub-domains Ω^+ and Ω^-, and Ω^- lies strictly in Ω;
$\mathbf{n}$: the unit normal direction of Γ pointing to Ω^+;
$\beta(\mathbf{x})$: a positive and piecewise constant, that is,

$$\beta(\mathbf{x}) = \beta^+ \text{ if } \mathbf{x} \in \Omega^+, \qquad \beta(\mathbf{x}) = \beta^- \text{ if } \mathbf{x} \in \Omega^-. \tag{59}$$

The weak formulation of the state equation is

$$\text{Find } y \in H_0^1(\Omega) \text{ such that } a(y, v) = (u, v)_{L^2(\Omega)} \quad \forall v \in H_0^1(\Omega), \tag{60}$$

where

$$a(y, v) = \sum_{s=\pm} \int_{\Omega^s} \beta^s \nabla y \cdot \nabla v d\mathbf{x}$$

and

$$(u, v)_{L^2(\Omega)} = \int_{\Omega} uv d\mathbf{x}.$$

Problem

$(\mathbf{P})$ *Consider the optimal control problem of minimizing*

$$J(y,u) = \frac{1}{2}\int_\Omega (y - y_d)^2 \, d\mathbf{x} + \frac{\alpha}{2}\int_\Omega u^2 \, d\mathbf{x} \tag{61}$$

over all $(y,u) \in H_0^1(\Omega) \times L^2(\Omega)$ *subject to the elliptic interface equation (56)-(58) and the control constraints*

$$u_a \le u \le u_b. \tag{62}$$

The regularization parameter α is a fixed positive number and the set of admissible controls for $(\mathbf{P})$ can be written as

$$U_{ad} = \{u \in L^2(\Omega) : u_a \le u \le u_b\}.$$

Optimal control problems governed by elliptic PDE:

- R. Li, W. Liu, and H. Ma. **Adaptive FEM...**, SIAM J. Control Optim.,2002.
- E. Casas and M. Mateos. **Maximum norm Error...**, Comput. Optim. Appl., 2008.
- Y. Chen, Y. Huang, W. Liu, N. Yan. **Error and superconvergence MFEM...**, J. Sci. compu. 2010.
- E. Casas, C. Clason, and K. Kunisch, **Error estimates for sparse solutions...**, SIAM J. Control Optim.,2012
- W. Gong, G. Wang, and N. Yan, **Error estimates on a Lower Dimensional Manifold...**, SIAM J. Control Optim., 2014
- Hui. Chang and D. Yang, **Domain decomposition method...**, J. Compu. Appl. Math., 2011
- T. Apel, J. Pfefferer, and A. Rösch. **Error estimates for Neumann...**, Comput. Optim. Appl., 2012.
- M. Hinze, R. Pinnau, M. Ulbrich, and S. Ulbrich, **Optimization with PDE Constraints. Math. Model. Theory Appl.**, Springer, 2009

Applications

• M. MU,**Nonlinear singular vectors and nonlinear singular values**, Science in China, Ser. D, 2000

• M. MU, Z. Zhang, **Conditional nonlinear optimal perturbations of a two-dimensional quasigeostrophic model**, J.Atmos.Sci., 2006

• ......

Optimal control problems governed by elliptic PDE with discontinuous coefficients:

• T. Apel and D. Sirch. A priori mesh grading for distributed optimal control problems. In Constrained Optimization and Optimal Control for Partial Differential Equations, pages 377 – 389. Springer, 2012.

• M. Hinze. A **variational discretization concept** in control constrained optimization: the linear-quadratic case. Comput. Optim. Appl., 30:45 – 61, 2005.

The problem $(\mathbf{P})$ admits a unique optimal control $u^* \in L^2(\Omega)$, with an associated state $y^* \in H_0^1(\Omega)$ and an adjoint state $p^* \in H_0^1(\Omega)$ that satisfy the state equation

$$a(y^*, v) = (u^*, v)_{L^2(\Omega)} \quad \forall v \in H_0^1(\Omega), \tag{63}$$

the adjoint equation

$$a(v, p^*) = (y^* - y_d, v)_{L^2(\Omega)} \quad \forall v \in H_0^1(\Omega), \tag{64}$$

and the variational inequality

$$(\alpha u^* + p^*, w - u^*)_{L^2(\Omega)} \geq 0 \quad \forall\ w \in U_{ad}. \tag{65}$$

Moreover, the variational inequality is equivalent to

$$u^* = \mathcal{P}_{[u_a, u_b]}(-\frac{1}{\alpha} p^*), \tag{66}$$

where $\mathcal{P}_{[u_a,u_b]}(v)$ denotes the projection of $v \in \mathbb{R}$ onto the interval $[u_a, u_b]$.

The adjoint equation

$$a(v, p^*) = (y^* - y_d, v)_{L^2(\Omega)} \quad \forall v \in H_0^1(\Omega), \tag{67}$$

is the weak form of the following interface problem

$$\begin{aligned} &-\nabla \cdot (\beta \nabla p) = y - y_d \quad \text{in } \Omega, \\ &p = 0 \text{ on } \partial\Omega, \\ &[p]_\Gamma = 0, [\beta \partial_{\mathbf{n}} p]_\Gamma = 0. \end{aligned} \tag{68}$$

Lemma

If the function $u \in L^2(\Omega)$ *and the interface* $\Gamma \in C^2$*, then the problem (56)-(58) has a unique solution* $y \in \widetilde{H}^2(\Omega) \cap H_0^1(\Omega)$ *which satisfies for some constant* $C > 0$

$$\|y\|_{\widetilde{H}^2(\Omega)} \le C\|u\|_{L^2(\Omega)}, \tag{69}$$

where

$$\widetilde{H}^2(\Omega) := \left\{ y \in H^1(\Omega) : \; y \in \widetilde{H}^2(\Omega^s), \; s = +, \; - \right\}$$

equipped with the norm $\|y\|^2_{\widetilde{H}^2(\Omega)} := \|y\|^2_{H^2(\Omega^+)} + \|y\|^2_{H^2(\Omega^-)}$.

Theorem

Let (u^*, y^*, p^*) *be the solutions of the problem* $(\mathbf{P})$*. Then we have*

$$(u^*, y^*, p^*) \in L^2(\Omega) \times \widetilde{H}^2(\Omega) \times \widetilde{H}^2(\Omega).$$

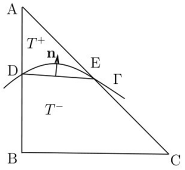

Fig.1: A typical interface element.

We construct the following piecewise linear function

$$\phi(x) = \begin{cases} \phi^+ = a^+ + b^+ x_1 + c^+ x_2, & \mathbf{x} = (x_1, x_2) \in T^+, \\ \phi^- = a^- + b^- x_1 + c^- x_2, & \mathbf{x} = (x_1, x_2) \in T^-, \end{cases} \tag{70}$$

where the coefficients are chosen such that

$$\phi(A) = V_1, \ \phi(B) = V_2, \ \phi(C) = V_3, \tag{71}$$

$$\phi^+(D) = \phi^-(D), \ \phi^+(E) = \phi^-(E), \ \beta^+ \partial_{\mathbf{n}} \phi^+ = \beta^- \partial_{\mathbf{n}} \phi^-. \tag{72}$$

Definition

(IFE space) The IFE space $V_h^J(\Omega)$ is defined as the set of all piecewise linear functions that satisfy

- $\phi|_T$ is the linear function if T is the non-interface element
- $\phi|_T$ is the piecewise linear function defined in (70)-(72) if T is the interface element
- ϕ is continuous at all nodal points,
- $\phi(\mathbf{x}_b) = 0$ if $\mathbf{x}_b$ is a nodal point on $\partial\Omega$.

Problem

(IFE approximation) For any $u \in L^2(\Omega)$, find $y_h \in V_h^J(\Omega)$ such that

$$a_h(y_h, v_h) = (u, v_h)_{L^2(\Omega)} \quad \forall v_h \in V_h^J(\Omega), \tag{73}$$

where

$$a_h(u, v) := \sum_{T \in \mathcal{T}_h} \int_T \beta \nabla u \cdot \nabla v dx \quad \forall u, v \in H_h(\Omega).$$

Lemma

(Discrete Poincaré inequality) There exists a constant C independent of h *and the interface* Γ *such that*

$$\|\phi\|_{L^2(\Omega)} \leq C a_h(\phi,\phi) \qquad \forall \phi \in V_h^J(\Omega). \tag{74}$$

Theorem

(Error estimates) Let $y \in \widetilde{H}^2(\Omega) \cap H_0^1(\Omega)$ *and* $y_h \in V_h^J(\Omega)$ *be the solutions of (56)-(58) and (73) respectively. Then there exists a constant* $C > 0$ *such that*

$$\|y - y_h\|_{1,h} \leq Ch\|y\|_{\widetilde{H}^2(\Omega)}, \tag{75}$$

$$\|y - y_h\|_{L^2(\Omega)} \leq Ch^2\|y\|_{\widetilde{H}^2(\Omega)}. \tag{76}$$

Problem

$(\mathbf{P_h})$ *Consider the problem of minimizing*

$$J_h(y_h, u) = \frac{1}{2}\int_\Omega (y_h - y_d)^2 d\mathbf{x} + \frac{\alpha}{2}\int_\Omega u^2 d\mathbf{x} \tag{77}$$

over all $(y_h, u) \in V_h^J(\Omega) \times L^2(\Omega)$ *subject to*

$$a_h(y_h, v_h) = (u, v_h)_{L^2(\Omega)} \qquad \forall v_h \in V_h^J(\Omega) \tag{78}$$

and the control constraints

$$u_a \le u \le u_b. \tag{79}$$

The problem $(\mathbf{P_h})$ has a unique solution $u_h^* \in L^2(\Omega)$ with associated state $y_h^* \in V_h^J(\Omega)$ and adjoint state $p_h^* \in V_h^J(\Omega)$ that satisfy the state equation

$$a_h(y_h^*, v_h) = (u_h^*, v_h)_{L^2(\Omega)} \qquad \forall v_h \in V_h^J(\Omega), \tag{80}$$

the adjoint equation

$$a_h(v_h, p_h^*) = (v_h, y_h^* - y_d)_{L^2(\Omega)} \quad \forall v_h \in V_h^J(\Omega), \tag{81}$$

and the projection equation

$$u_h^* = \mathcal{P}_{[u_a, u_b]}(-\frac{1}{\alpha} p_h^*). \tag{82}$$

The projection equation is equivalent to the variational inequality

$$(\alpha u_h^* + p_h^*, w - u_h^*)_{L^2(\Omega)} \geq 0 \quad \forall w \in U_{ad}. \tag{83}$$

To get error estimates between $(\mathbf{P})$ and $(\mathbf{P_h})$, we introduce the auxiliary functions $y^h \in V_h^J(\Omega)$ and $p^h \in V_h^J(\Omega)$ which are solutions of the following problems

$$a_h(y^h, v_h) = (u^*, v_h)_{L^2(\Omega)} \quad \forall v_h \in V_h^J(\Omega), \tag{84}$$

$$a_h(v_h, p^h) = (v_h, y^* - y_d)_{L^2(\Omega)} \quad \forall v_h \in V_h^J(\Omega). \tag{85}$$

There exists a constant $C > 0$, independent of h, such that

$$\|y^* - y^h\|_{L^2(\Omega)} \leq Ch^2, \quad \|y^* - y^h\|_{1,h} \leq Ch, \tag{86}$$

$$\|p^* - p^h\|_{L^2(\Omega)} \leq Ch^2, \quad \|p^* - p^h\|_{1,h} \leq Ch. \tag{87}$$

Theorem

Let (u^*, y^*, p^*) *and* (u_h^*, y_h^*, p_h^*) *be the solutions of the problems* (P) *and* (P_h) *respectively. Then there exists a constant* $C > 0$*, independent of* h*, such that*

$$\alpha\|u^* - u_h^*\|_{L^2(\Omega)}^2 + \|y^* - y_h^*\|_{L^2(\Omega)}^2 \leq \frac{1}{\alpha}\|p^* - p^h\|_{L^2(\Omega)}^2 + \|y^* - y^h\|_{L^2(\Omega)}^2, \tag{88}$$

$$|y^* - y_h^*|_{1,h}^2 \leq C\left(\|y^* - y^h\|_{1,h}^2 + \|u^* - u_h^*\|_{L^2(\Omega)}^2\right), \tag{89}$$

$$\|p^* - p_h^*\|_{L^2(\Omega)}^2 \leq C\left(\|p^* - p^h\|_{L^2(\Omega)}^2 + \|y^* - y_h^*\|_{L^2(\Omega)}^2\right), \tag{90}$$

$$|p^* - p_h^*|_{1,h}^2 \leq C\left(\|p^* - p^h\|_{1,h}^2 + \|y^* - y_h^*\|_{L^2(\Omega)}^2\right). \tag{91}$$

Theorem

Let (u^*, y^*, p^*) and (u_h^*, y_h^*, p_h^*) be the solutions of the optimal control problem (P) and (P_h) respectively. Then there exists a generic constant C, independent of the mesh size h, such that

$$\|u^* - u_h^*\|_{L^2(\Omega)} \leq Ch^2, \quad \|y^* - y_h^*\|_{L^2(\Omega)} \leq Ch^2, \quad |y^* - y_h^*|_{1,h} \leq Ch, \tag{92}$$

$$\|p^* - p_h^*\|_{L^2(\Omega)} \leq Ch^2, \quad |p^* - p_h^*|_{1,h} \leq Ch. \tag{93}$$

Remark: In the case of $U_{ad} = L^2(\Omega)$ (unconstrained problem), the projection equations become $u^* = -\frac{1}{\alpha}p^*$ and $u_h^* = -\frac{1}{\alpha}p_h^*$, respectively. Using the properties of $p*$ and p_h^*, we then have the regularity of the control $u^* \in \widetilde{H}^2(\Omega)$ and the following H^1 error estimate

$$|u^* - u_h^*|_{1,h} \leq Ch.$$

We consider in the sequel a general problem where the state equation of the problem $(\mathbf{P})$ is replaced by

$$\begin{aligned} & -\nabla\cdot(\beta\nabla y) = f + u \quad \text{ in } \Omega\backslash\Gamma, \\ & y = g \quad \text{ on } \partial\Omega, \\ & [y]_\Gamma = 0, \;\; [\beta\partial_{\mathbf{n}} y]_\Gamma = 0. \end{aligned} \tag{94}$$

In order to find the solution of the problem $(\mathbf{P_h})$, we then have to solve the coupled problem

$$a_h(y_h^*, v_h) = (f + u_h^*, v_h)_{L^2(\Omega)} \qquad \forall v_h \in V_h^J(\Omega), \tag{95}$$

$$a_h(v_h, p_h^*) = (v_h, y_h^* - y_d)_{L^2(\Omega)} \qquad \forall v_h \in V_h^J(\Omega), \tag{96}$$

$$u_h^* = \mathcal{P}_{[u_a, u_b]}\left(-\frac{1}{\alpha} p_h^*\right). \tag{97}$$

Note that the function $y_h^* \in V_{h,g}^J(\Omega)$ satisfies the discrete boundary condition. Let $\{\phi_1, \cdots, \phi_m\}$ be basis functions of $V_h^J(\Omega)$.

For the boundary condition to be satisfied, we also define functions $\phi_{m+1}, \cdots, \phi_{m+l}$ so that $\sum_{j=m+1}^{m+l} g(\mathbf{x}_j)\phi_j$ interpolates the boundary data. The function y_h^* then can be written as

$$y_h^* = \sum_{j=1}^{m} Y(j)\phi_j + \sum_{j=m+1}^{m+l} g(\mathbf{x}_j)\phi_j. \tag{98}$$

We get the matrix-vector form of the state equation

$$AY = F_1 + MU, \tag{99}$$

where

$$A(i,j) = a_h(\phi_j, \phi_i),\ \ Y(j) = y_h^*(\mathbf{x}_j),\ \ M(i,j) = (\phi_j, \phi_i)_{L^2(\Omega)}, U(j) = u_h^*(\mathbf{x}_j),$$

$$F_1(i) = (f, \phi_i)_{L^2(\Omega)} - \sum_{j=m+1}^{m+l} g(\mathbf{x}_j) a_h(\phi_j, \phi_i), \quad i, j = 1, \cdots, m. \tag{100}$$

Similarly, we obtain the matrix-vector form of the adjoint equation,

$$AP = MY + F_2, \tag{101}$$

where

$$P(j) = p_h^*(\mathbf{x}_j), \quad F_2(i) = -(y_d, \phi_i)_{L^2(\Omega)}, \quad i, j = 1, \cdots, m. \tag{102}$$

In the case of $U_{ad} = L^2(\Omega)$, the projection equation $u_h^* = \mathcal{P}_{[u_a,u_b]}\left(-\frac{1}{\alpha}p_h^*\right)$ becomes

$$u_h^* = -\frac{1}{\alpha}p_h^*. \tag{103}$$

The vector form is $U = -\frac{1}{\alpha}P$. Therefore we have the following large linear system of equations (saddle point problem)

$$\begin{bmatrix} -\alpha M & \mathbf{0} & -M \\ \mathbf{0} & -M & A \\ -M & A & \mathbf{0} \end{bmatrix} \begin{bmatrix} U \\ Y \\ P \end{bmatrix} = \begin{bmatrix} \mathbf{0} \\ F_2 \\ F_1 \end{bmatrix}. \tag{104}$$

The system of equations is symmetric but indefinite, so we solve it using the MINRES method.

In order to get a satisfactory convergence, a block diagonally preconditioner is applied, that is,

$$\begin{bmatrix} \alpha M & \mathbf{0} & \mathbf{0} \\ \mathbf{0} & M & \mathbf{0} \\ \mathbf{0} & \mathbf{0} & AM^{-1}A \end{bmatrix}. \tag{105}$$

In the case of $U_{ad} = \{u \in L^2(\Omega) : u_a \le u \le u_b\}$, $(\mathbf{P_h})$ leads to a single equation for the optimal control u_h^*,

$$G(u) := u - \mathcal{P}_{[u_a,u_b]}\left(-\frac{1}{\alpha}p_h(u)\right) = 0, \tag{106}$$

A fix-point iteration algorithm is used to solve the nonlinear and non-smooth equation.

Algorithm

1. Give an initial function $u_0 \in L^2(\Omega)$.
2. Get $y_h \in V_h^J(\Omega)$ by solving $a_h(y_h, v_h) = (f + u_0, v_h)_{L^2(\Omega)}\ \forall v_h \in V_h^J(\Omega)$.
3. Get $p_h \in V_h^J(\Omega)$ by solving
$a_h(v_h, p_h) = (v_h, y_h - y_d)_{L^2(\Omega)}\ \forall v_h \in V_h^J(\Omega)$.
4. Get u_1 by the equation $u_1 = \mathcal{P}_{[u_a,u_b]}\left(-\frac{1}{\alpha}p_h\right)$, where
$\mathcal{P}_{[a,b]}(v(\mathbf{x})) := \max\{a, \min\{v(\mathbf{x}), b\}\}$.
5. If $|u_0 - u_1| \le 1.0 \times 10^{-6}$, then we set $u_h^* = u_1$, else we set $u_0 = u_1$ and goto step 2.

Example 1. We set $U_{ad} = L^2(\Omega)$. The interface is a circle centered at the origin with radius $r_0 = 0.5$. Let

$$u^*(\mathbf{x}) = \begin{cases} \dfrac{(x_1^2 + x_2^2 - r_0^2)(x_1 - 1)(x_1 + 1)(x_2 - 1)(x_2 + 1)}{\beta^-} & \text{in } \Omega^-, \\[2ex] \dfrac{(x_1^2 + x_2^2 - r_0^2)(x_1 - 1)(x_1 + 1)(x_2 - 1)(x_2 + 1)}{\beta^+} & \text{in } \Omega^+, \end{cases} \tag{107}$$

Then we have $p^* = -\alpha u^*$. It is easy to verify that p^* satisfies the interface jump conditions and the homogeneous Dirichlet boundary condition in (68). We choose

$$y^*(\mathbf{x}) = \begin{cases} \dfrac{(x_1^2 + x_2^2)^{3/2}}{\beta^-} & \text{in } \Omega^-, \\[2ex] \dfrac{(x_1^2 + x_2^2)^{3/2}}{\beta^+} + \left(\dfrac{1}{\beta^-} - \dfrac{1}{\beta^+}\right) r_0^3 & \text{in } \Omega^+. \end{cases} \tag{108}$$

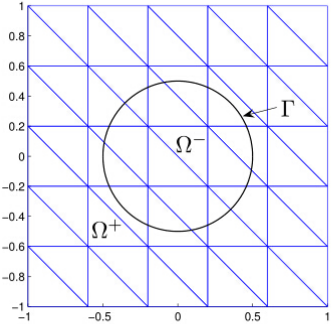

Fig.2: The geometry of the domain and the interface. A triangulation with N=5 is plotted.

(a) Errors in the L^2-norm

N	$\|u^* - u_h^*\|_{L^2(\Omega)}$	Order	$\|y^* - y_h^*\|_{L^2(\Omega)}$	Order	$\|p^* - p_h^*\|_{L^2(\Omega)}$	Order
16	5.1370E-03		4.1030E-03		5.1370E-05	
32	1.3368E-03	1.94	1.1277E-03	1.86	1.3368E-05	1.94
64	3.0153E-04	2.14	3.0882E-04	1.86	3.0153E-06	2.14
128	6.4095E-05	2.23	6.7483E-05	2.19	6.4095E-07	2.23
256	1.3788E-05	2.21	1.5963E-05	2.07	1.3788E-07	2.21

(b) Errors in the H^1-norm

N	$\|u^* - u_h^*\|_{1,h}$	Order	$\|y^* - y_h^*\|_{1,h}$	Order	$\|p^* - p_h^*\|_{1,h}$	Order
16	1.0446E-01		7.7461E-02		1.0446E-03	
32	4.4963E-02	1.21	3.9848E-02	0.95	4.4963E-04	1.21
64	2.1327E-02	1.07	2.0029E-02	0.99	2.1327E-04	1.07
128	1.0345E-02	1.04	9.9818E-03	1.00	1.0345E-04	1.04
256	5.1766E-03	0.99	5.0257E-03	0.98	5.1766E-05	0.99

Table.1: Grid refinement analysis for Example 1 with $\beta^- = 1$, $\beta^+ = 1000$.

(a) Errors in the L^2-norm

N	$\|u^* - u_h^*\|_{L^2(\Omega)}$	Order	$\|y^* - y_h^*\|_{L^2(\Omega)}$	Order	$\|p^* - p_h^*\|_{L^2(\Omega)}$	Order
16	5.2229E-02		1.7588E-02		5.2229E-04	
32	1.3346E-02	1.96	4.3994E-03	1.99	1.3346E-04	1.96
64	3.3636E-03	1.98	1.0960E-03	2.00	3.3636E-05	1.98
128	8.4054E-04	2.00	2.7649E-04	1.98	8.4054E-06	2.00
256	2.0943E-04	2.00	6.9620E-05	1.98	2.0943E-06	2.00

(b) Errors in the H^1-norm

N	$\|u^* - u_h^*\|_{1,h}$	Order	$\|y^* - y_h^*\|_{1,h}$	Order	$\|p^* - p_h^*\|_{1,h}$	Order
16	3.8286E-01		3.9971E-01		3.8286E-03	
32	1.6997E-01	1.17	2.0010E-01	0.99	1.6997E-03	1.17
64	8.1876E-02	1.05	1.0009E-01	0.99	8.1876E-04	1.05
128	4.0523E-02	1.01	5.0045E-02	1.00	4.0523E-04	1.01
256	2.0210E-02	1.00	2.5027E-02	0.99	2.0210E-04	1.00

Table.2: Grid refinement analysis for Example 1 with $\beta^- = 1000$, $\beta^+ = 1$.

(a) Errors in the L^2-norm

N	$\|u^* - u_h^*\|_{L^2(\Omega)}$	Order	$\|y^* - y_h^*\|_{L^2(\Omega)}$	Order	$\|p^* - p_h^*\|_{L^2(\Omega)}$	Order
16	1.1889E-02		4.6400E-03		1.1889E-04	
32	3.1406E-03	1.92	1.2288E-03	1.91	3.1406E-05	1.92
64	7.0663E-04	2.15	3.1438E-04	1.96	7.0663E-06	2.15
128	1.6334E-04	2.11	8.1934E-05	1.93	1.6334E-06	2.11
256	3.5894E-05	2.18	2.1650E-05	1.92	3.5894E-07	2.18

(b) Errors in the H^1-norm

N	$\|u^* - u_h^*\|_{1,h}$	Order	$\|y^* - y_h^*\|_{1,h}$	Order	$\|p^* - p_h^*\|_{1,h}$	Order
16	1.0665E-01		1.0778E-01		1.0665E-03	
32	5.2602E-02	1.01	5.5660E-02	0.95	5.2602E-04	1.01
64	2.7054E-02	0.95	2.9084E-02	0.93	2.7054E-04	0.95
128	1.4028E-02	0.94	1.5047E-02	0.95	1.4028E-04	0.94
256	7.4170E-03	0.91	7.9081E-03	0.92	7.4170E-05	0.91

Table.3: Grid refinement analysis for Example 1 with $\beta^- = 1$, $\beta^+ = 5$.

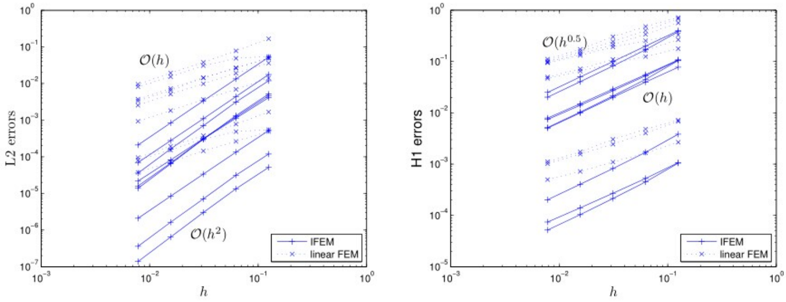

Fig.3: Errors of control, state, and adjoint state plotted against mesh size h for Example 1 with different β^- and β^+. Left: L^2-errors. Right: H^1-errors. The IFEM achieves optimal convergence, but the standard linear FEM does not.

Example 2. The interface is also a circle centered at the origin with radius $r_0 = 0.5$. The space $U_{ad} = \{u \in L^2(\Omega) : u_a \leq u \leq u_b\}$. In this example, we choose $u_a = -1$, $u_b = 1$ and $\alpha = 1$. In order to construct exact solutions, we first give a function which satisfies the interface conditions and the homogeneous boundary condition,

$$\varphi(\mathbf{x}) = \begin{cases} \dfrac{5(x_1^2 + x_2^2 - r_0^2)(x_1 - 1)(x_1 + 1)(x_2 - 1)(x_2 + 1)}{\beta^-} & \text{in } \Omega^-, \\[2ex] \dfrac{5(x_1^2 + x_2^2 - r_0^2)(x_1 - 1)(x_1 + 1)(x_2 - 1)(x_2 + 1)}{\beta^+} & \text{in } \Omega^+. \end{cases}$$

Then we set the optimal control and the associated state by

$$\begin{aligned} u^*(\mathbf{x}) &= \mathcal{P}_{[-1,1]}(\varphi(\mathbf{x})) = \min\{1, \max\{-1, \varphi(\mathbf{x})\}\}, \\ p^*(\mathbf{x}) &= -\alpha\varphi(\mathbf{x}). \end{aligned} \tag{109}$$

We also take the optimal state as

$$y^*(\mathbf{x}) = \begin{cases} \dfrac{(x_1^2+x_2^2)^{3/2}}{\beta^-} & \text{in } \Omega^-, \\[2ex] \dfrac{(x_1^2+x_2^2)^{3/2}}{\beta^+} + \left(\dfrac{1}{\beta^-} - \dfrac{1}{\beta^+}\right) r_0^3 & \text{in } \Omega^+. \end{cases}$$

Then we can determine the functions f, g and y_d accordingly. We fix $\beta^- = 1$ so that the active set D is not empty, where $D := \{\mathbf{x} \in \Omega : u^*(\mathbf{x}) = u_a \text{ or } u^*(\mathbf{x}) = u_b\}$.

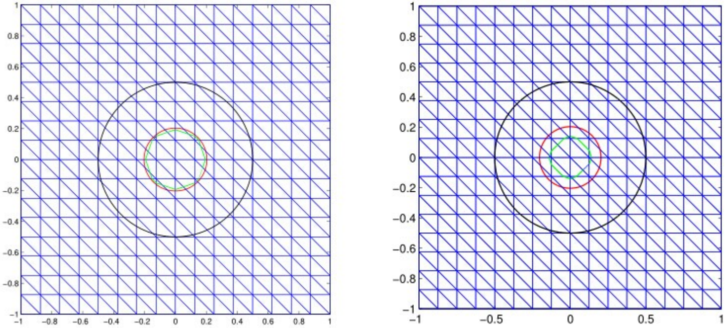

(a) IFEM (b) Standard linear FEM

Fig.4: The geometry of Example 2 with $\beta^+ = 5$. The black, red and green curves depict the interface, the exact border of the active set D, the discrete border obtained by the IFEM (left) and the standard linear FEM (right) with N=16, respectively.

(a) Errors in the L^2-norm

N	$\|u^* - u_h^*\|_{L^2(\Omega)}$	Order	$\|y^* - y_h^*\|_{L^2(\Omega)}$	Order	$\|p^* - p_h^*\|_{L^2(\Omega)}$	Order
16	2.0049E-02		5.6594E-03		2.5823E-02	
32	5.4877E-03	1.86	1.4803E-03	1.93	6.6744E-03	1.95
64	1.4215E-03	1.94	3.6993E-04	2.00	1.6418E-03	2.02
128	3.6148E-04	1.97	9.4048E-05	1.97	4.0256E-04	2.02
256	9.6419E-05	1.90	2.2873E-05	2.03	1.0293E-04	1.96

(b) Errors in the H^1-norm

N	$\|y^* - y_h^*\|_{1,h}$	Order	$\|p^* - p_h^*\|_{1,h}$	Order
16	1.0772E-01		5.0950E-01	
32	5.5662E-02	0.95	2.6007E-01	0.97
64	2.9088E-02	0.93	1.3522E-01	0.94
128	1.5048E-02	0.95	7.0160E-02	0.94
256	7.9084E-03	0.92	3.7090E-02	0.91

Table.4: Grid refinement analysis for Example 2 with $\beta^- = 1$, $\beta^+ = 5$.

(a) Errors in the L^2-norm

N	$\|u^* - u_h^*\|_{L^2(\Omega)}$	Order	$\|y^* - y_h^*\|_{L^2(\Omega)}$	Order	$\|p^* - p_h^*\|_{L^2(\Omega)}$	Order
16	1.6780E-02		4.9160E-03		2.6095E-02	
32	4.4343E-03	1.91	1.3109E-03	1.90	5.9808E-03	2.12
64	1.1998E-03	1.88	3.5248E-04	1.89	1.4726E-03	2.02
128	2.5332E-04	2.24	7.9136E-05	2.15	3.1414E-04	2.22
256	5.9177E-05	2.09	1.8361E-05	2.10	7.3014E-05	2.10

(b) Errors in the H^1-norm

N	$\|y^* - y_h^*\|_{1,h}$	Order	$\|p^* - p_h^*\|_{1,h}$	Order
16	7.7737E-02		4.7523E-01	
32	3.9893E-02	0.96	2.1832E-01	1.12
64	2.0038E-02	0.99	1.0621E-01	1.03
128	9.9826E-03	1.00	5.1660E-02	1.03
256	5.0258E-03	0.99	2.5877E-02	0.99

Table.5: Grid refinement analysis for Example 2 with $\beta^- = 1$, $\beta^+ = 1000$.

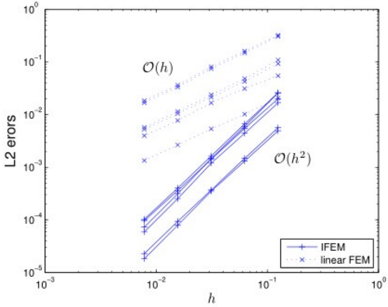

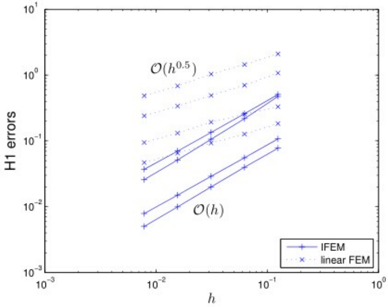

Fig.5: Errors of control, state, and adjoint state plotted against mesh size h for Example 2 with $\beta^+ = 5$ and $\beta^+ = 1000$. Left: L^2-errors. Right: H^1-errors. The IFEM achieves optimal convergence, but the standard linear FEM does not.

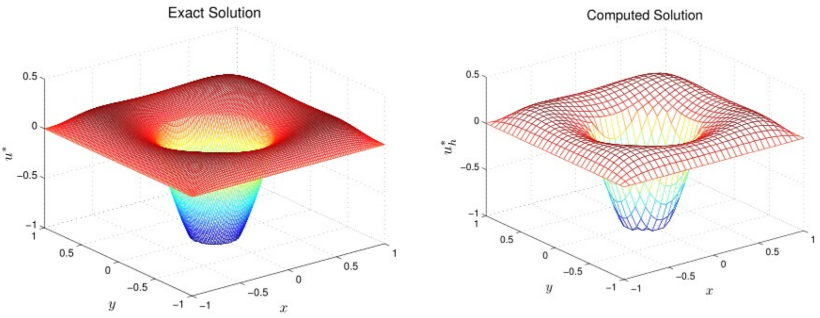

Fig.6: The exact control and the discrete control obtained by the IFEM with N=32 for Example 2 with $\beta^+ = 5$.

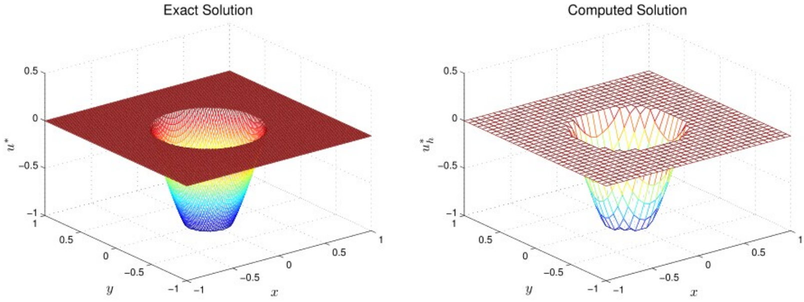

Fig.7: The exact control and the discrete control obtained by the IFEM with N=32 for Example 2 with $\beta^+ = 1000$.

Example 3: In this example, we use a more complicated interface, a 5-star interface, which is the zero level set of the function

$$\varphi(\mathbf{x}) = r - (0.5 + 0.2\sin(5\theta)),$$

where (r, θ) is the polar coordinate representation of $\mathbf{x}$. We set $f(\mathbf{x}) = 0$, $g = 0$, $y_d(\mathbf{x}) = 1$ and the regularization parameter $\alpha = 1.0 \times 10^{-4}$.

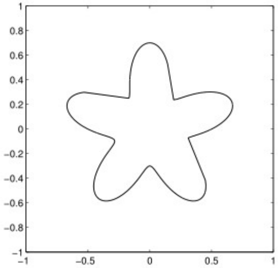

Fig.8: A plot of the 5-star interface.

This model problem can be interpreted as optimization of a stationary heating process in composite media.
β: the thermal conductivity of the different media and the function,
$f(\mathbf{x})$: an external heat source.
The optimal control problem is to find the proper heat source (control u) to control the temperature of the composite media to maintain the same everywhere (desired state $y_d = 1$).
We test three cases: $\beta^+/\beta^- = 10/1$, $\beta^+/\beta^- = 1/1$ and $\beta^+/\beta^- = 1/10$.

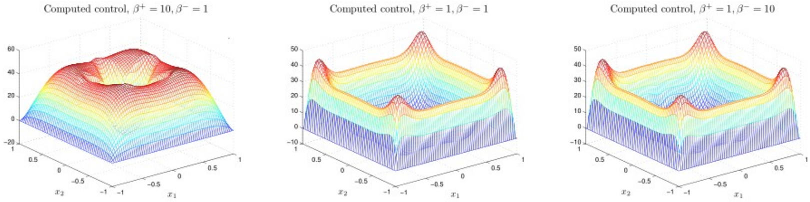

Fig.9: The computed controls for Example 3 with different coefficients.

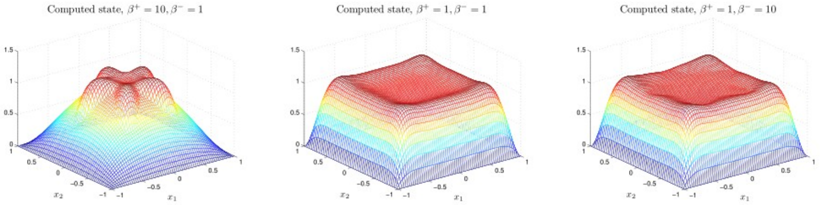

Fig.10: The computed states for Example 3 with different coefficients.

Example 4: As the previous example, we also use the 5-star as the interface, while the corresponding data are changed:
$y_d(\mathbf{x}) = (1 - x_1^2)(1 - x_2^2)$, $g = 0$, and

$$f(\mathbf{x}) = \begin{cases} \nabla \cdot (\beta^+ \nabla y_d(\mathbf{x})) & \text{if } \mathbf{x} \in \Omega^+, \\ \nabla \cdot (\beta^- \nabla y_d(\mathbf{x})) & \text{if } \mathbf{x} \in \Omega^-. \end{cases} \tag{110}$$

Note that if $\beta^+ = \beta^-$, then it is easy to verify that the optimal control $u^* = 0$, the state $y^* = y_d$ (the interface conditions (57) hold) and the objective function $J(y^*, u^*) = 0$. However, if $\beta^+ \neq \beta^-$, then it is hard to get the optimal control intuitively even if (55) holds. The aim of this example is to investigate the shape of the optimal control and the corresponding state when $\beta^+ \neq \beta^-$. Without loss of generality, we set $\beta^+ = 10$ and $\beta^- = 1$.

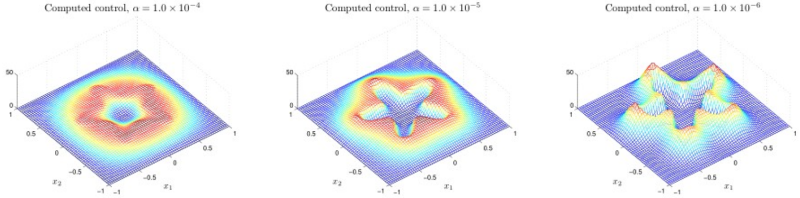

Fig.11: The computed controls for Example 4 with the regularization parameter $\alpha = 1.0 \times 10^{-4}, 1.0 \times 10^{-5}$ and 1.0×10^{-6}.

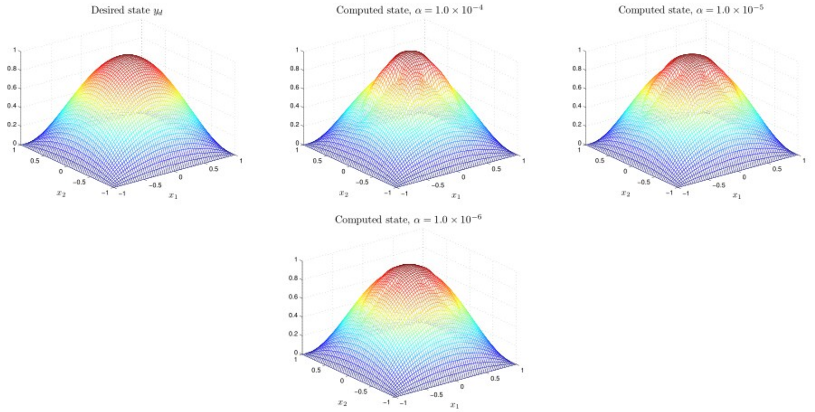

Fig.12: The desired state y_d and the computed states for Example 4 with the regularization parameter $\alpha = 1.0 \times 10^{-4}, 1.0 \times 10^{-5}$ and 1.0×10^{-6}.

Example 5. We change the Example 4 to a constrained one. The control is restricted by box constraints $u_a \leq u \leq u_b$ with $u_a = -5$ and $u_b = 5$.

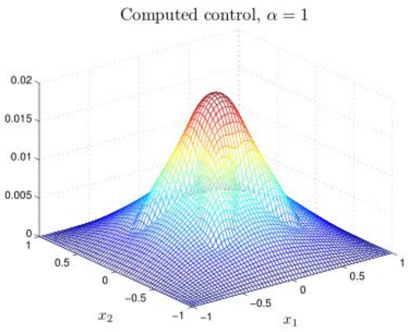

Fig.13: The computed controls for Example 5 with the regularization parameter $\alpha = 1.0$ and 2.0×10^{-3}.

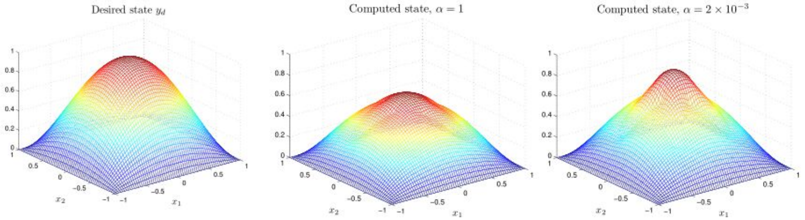

Fig.14: The desired state y_d and the computed states for Example 5 with the regularization parameter $\alpha = 1$ and 2.0×10^{-3}.

1. An unfitted mesh independent of the shape and location of the interface is used.
2. On interface elements the basis functions are modified to satisfy the interface conditions.
3. The accuracy of our method remains the same as that of standard methods.
4. Optimal error estimates are derived and numerical examples are provided.

References:

1. L. Zhu, Z.Y. Zhang and Z.L. Li, The immersed finite volume element method for some interface problems with nonhomogenous jump conditions, **International Journal of Numerical Analysis and Modeling**, 2016, 13(3):368-382.

2. L. Zhu, Z.L. Li and Z.Y. Zhang, An immersed finite volume element method for 2D PDEs with discontinuous coefficients and non-homogeneous jump conditions, **Computers and Mathematics with Applications**, 2015, 70:89-103.

3. Q. Zhang, Z.L. Li, and Z.Y. Zhang, A sparse grid stochastic collocation method for elliptic interface problems with random input, **Journal of Scientific Computing**, 2016,67:262-280.

4. Q. Zhang, K. Ito, Z.L. Li and Z.Y. Zhang, Immersed finite elements for optimal control problems of elliptic PDEs with interfaces, **Journal of Computational Physics**, 2015, 298:305-319.

Thank you!